

Ferromagnetism and spin-orbital compensation in Sm intermetallics

H. J. Gotsis* and I. I. Mazin

Code 6390, Center for Computational Materials Science, Naval Research Laboratory, Washington, DC 20375

(Received 31 July 2003; published 24 December 2003)

The electronic structure and magnetic properties of the ferromagnetic Sm intermetallics SmAl₂ and SmZn have been calculated within the local density approximation (LDA)+*U* method. In contrast to LDA, which predicts a strong peak of 4*f* character in the density of states on the Fermi level, the LDA+*U* method predicts occupied 4*f* states well below the Fermi energy and empty ones well above this energy. We find a sizeable orbital magnetic moment, comparable in magnitude with the opposite oriented spin moment. This result is consistent with the recent observation of ferromagnetic spin ordering, compensated by the orbital magnetization.

DOI: 10.1103/PhysRevB.68.224427

PACS number(s): 75.50.Cc, 71.20.Eh

I. INTRODUCTION

The ferromagnetic Sm intermetallics, the cubic (*C15*) Laves phase compound SmAl₂ and the CsCl-type compound SmZn, have attracted much attention because of the unique magnetic properties of Sm ions.¹⁻³ The spin and orbital magnetic moments, each having a different temperature dependence, nearly cancel each other.^{1,2} For gadolinium-doped SmAl₂ the cancellation is perfect at a compensation temperature T_{comp} of 67.5 K.³ At T_{comp} magnetic Compton scattering shows a net spin moment. The result is a material whose atoms and spins are aligned similar to those in a ferromagnet but produces no magnetic field. So SmAl₂ could be used in a unique spin-sensitive, nonmagnetic device, for instance, in a spin-polarized scanning tunneling microscope.³ Thermomagnetic curves of the ferromagnetic Sm intermetallics have been measured in a temperature range from 2 to 300 K.¹ Analysis of the results, using a single-ion Hamiltonian for the 4*f* electrons, gave the total ordered moment and the 4*f* spin, 4*f* orbital, and non-*f* conduction-electron components at 0 K. The three components to the site magnetization almost cancel, leaving a small net local moment.¹ An interesting experimental study of the magnetization density of Sm_{0.982}Gd_{0.018}Al₂ was reported recently.⁴ In this work non-resonant ferromagnetic x-ray diffraction was used to separate the spin and orbital contribution to the magnetization density of the proposed nonmagnetic ferromagnet Sm_{0.982}Gd_{0.018}Al₂.² For the net moment to be zero, the spin moment must be exactly compensated by the orbital moment. It was demonstrated in Ref. 4 that this compensation is driven by the different temperature dependencies of the spin and orbital parts. At the wave vector sampled, the conduction electron moment makes no contribution to the form factor, therefore their technique gives direct access to the temperature dependence of the spin and orbital components of the 4*f* moment. Below T_{comp} the orbital moment exceeds the spin one, while above T_{comp} they approximately cancel each other. Their result conclusively proves that the compensation mechanism is driven by the different temperature dependence of the Sm 4*f* spin and orbital moments. Specific heat data indicate that at T_{comp} the material exhibits no sign of magnetic transition. Therefore, the system remains ferromag-

netically ordered through T_{comp} . Furthermore, above T_{comp} the measured form factor is negligible. Thus it is reasonable to assume that the net magnetization observed above T_{comp} results almost exclusively from the conduction electron spin moment. Form factor measurements are not sensitive to this delocalized contribution. Such a measurement is planned using the magnetic Compton scattering technique, which directly samples the polarization of all spin polarized electrons.⁴ Photoemission (PE) spectroscopy using synchrotron radiation has revealed a pronounced difference in the magnitude of the surface core-level binding energy shifts between trivalent and divalent rare earth dialuminides.⁵ The divalent (including mixed-valent) exhibit much larger chemical shifts than the trivalent due to the high heat of formation for trivalent metallic rare earth compounds. The valence band PE spectrum of SmAl₂ contains a 4*f*⁵ final state multiplet close to the Fermi level (E_F) and a deeper lying 4*f*⁴ final state multiplet from bulk trivalent Sm ions. A 4*f*⁵ emission near E_F , originating from divalent Sm ions, clearly shows the existence of a surface induced valence transition in SmAl₂.⁵

However, neither the band structure nor the magnetic properties of SmAl₂ and SmZn have been studied theoretically yet. Therefore, a systematic investigation on the electronic and magnetic structures of Sm intermetallics is required. In this paper, we report the band structure calculations performed both in the local spin-density approximation (LSDA) and the LSDA+*U* incorporating spin-orbit coupling and compare the results with the experiment.

II. COMPUTATIONAL DETAILS

SmAl₂ crystallizes in the cubic $Fd\bar{3}m$ structure (space group No. 227) and therefore it belongs to the large class of Laves phase compounds. The unit cell consists of two formula units (i.e., six atoms). The experimental lattice parameter is 7.943 Å.¹ SmZn occurs in the CsCl structure (space group $Pm\bar{3}m$). The experimentally measured lattice constant is 3.64 Å.¹ The simple crystal structure of SmZn makes it an interesting material in computational treatment of Sm intermetallics.

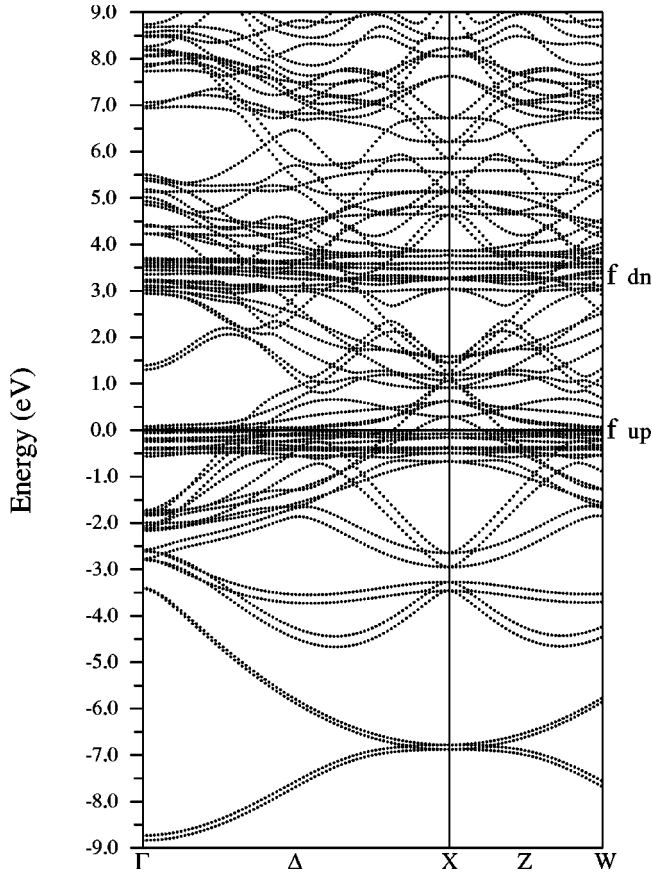


FIG. 1. Calculated band structure of SmAl_2 with the LSDA+SO approach.

One always faces difficulties in dealing with the band structure of f electron materials using the LSDA band calculations. This is due to the localized nature of f electrons as well as to the subtle interplay between the spin polarization and the spin-orbit interaction. The orbital magnetic moment is caused by the spin-orbit coupling and also by the many body correlation effects with the latter being more important. Since the Coulomb correlations in the Sm $4f$ shell is expected to be significant in these systems, the LSDA+ U method will be useful. The LSDA+ U ,⁶ removes the deficiency of LSDA by incorporating the Hubbard like interaction term for $4f$ electrons. To determine the size of orbital magnetic moments, we have explicitly included the spin-orbit coupling in the Hamiltonian. In this way, our calculational scheme corresponds to a relativistic LSDA+ U +SO method. It has been shown that the LSDA+ U method describes properly the orbital magnetism of solids with strongly correlated electrons.⁷ The LSDA+ U scheme was implemented in the fully localized form, which is appropriate for strongly localized electrons.⁸

The calculations were done using the general potential linearized augmented plane wave (LAPW) method,⁹ as implemented in the WIEN2K code.¹⁰ Both core and valence states are calculated self-consistently, the core states fully relativistically for the spherical part of the potential, and the valence states using the full potential. We used the muffin tin (MT) spheres $R_{\text{MT}}^{\text{Sm}}=2.5$ a.u., $R_{\text{MT}}^{\text{Al}}=2.6$ a.u. for SmAl_2 , and

TABLE I. The calculated magnetic moments and f occupation numbers of SmAl_2 . The $U=0/J=0$ represents an LSDA+SO calculation. The total spin magnetic moment/cell is given by m_{total} , the $4f$ orbital magnetic moment of the Sm atom is given by m_{orb} and the $4f$ spin moment of the Sm atom is given by m_{spin} . The f occupation numbers for $m=+1, +2, +3$ are given by n_{+1}, n_{+2} , and n_{+3} , respectively, for the other magnetic quantum numbers the occupancies are ≈ 1 .

U (Ry)	0.0	0/J=0	0.2	0.4	0.5	0.6
m_{total} (μ_B)	11.50	11.57	11.42	11.44	10.89	10.99
m_{orb} (μ_B)	-2.57	-2.37	-3.80	-4.28	-4.78	-4.85
m_{spin} (μ_B)	5.27	5.34	5.29	5.15	4.94	4.92
n_{+1}	0.65	0.78	0.95	0.97	0.98	0.98
n_{+2}	0.58	0.67	0.49	0.29	0.03	0.01
n_{+3}	0.41	0.32	0.02	0.01	0.02	0.01

$R_{\text{MT}}=2.0$ a.u. for SmZn . The basis sets were determined by a plane wave cutoff of $R_{\text{MT}}*K_{\text{max}}=7.0$ for SmAl_2 and $R_{\text{MT}}*K_{\text{max}}=9.0$ for SmZn , which give good convergence. Local orbitals were added in order to improve convergence and relax remaining linearization errors. Furthermore, for Sm we used a relativistic $p_{1/2}$ local orbital.¹¹ For the exchange-correlation potential we used the LSD approximation and the GGA functional of Perdew-Burke-Ernzerhof.¹² We used 13 k points in the irreducible wedge of the Brillouin zone (BZ) for SmAl_2 (convergence was checked by varying the number of

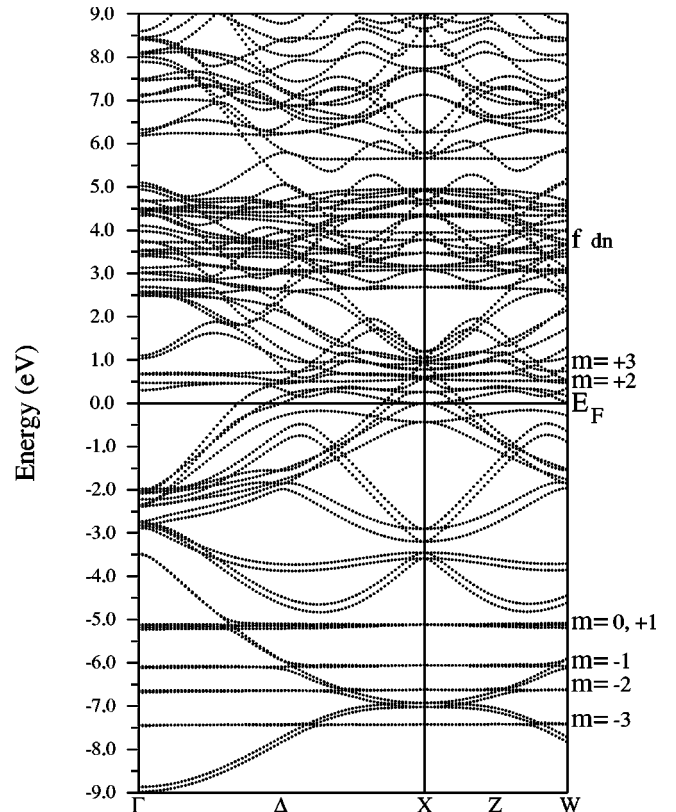


FIG. 2. Calculated band structure of SmAl_2 with the LSDA+ U +SO method.

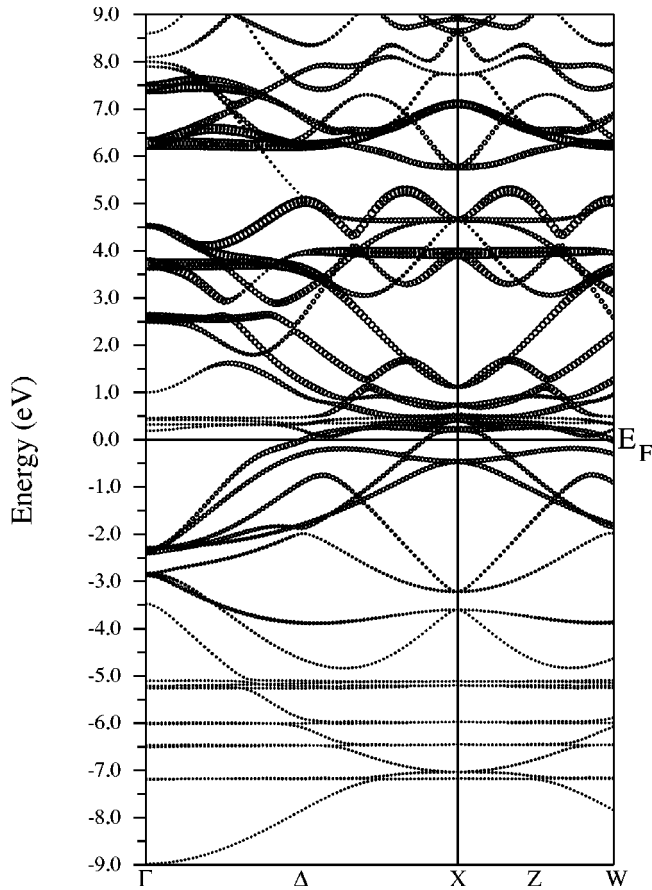


FIG. 3. The spin-up SmAl_2 band structure, obtained from the LSDA+ U calculation. The radius of the plotting circles is proportional to Sm d projection of the band.

k points, up to 30) and 40 k points for SmZn . Two main parameters in the LSDA+ U are the Hubbard U and the intra-atomic exchange J . We calculated these parameters from first principles, using the pseudoatomic loop of an LMTO code.¹³ (This approach usually results in smaller U than the con-

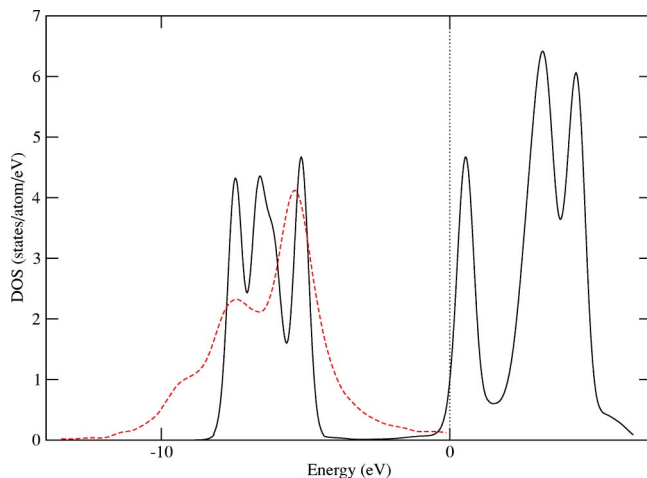


FIG. 4. The solid line is the calculated Sm $4f$ DOS, whereas the dashed line is the Sm $4f$ PE spectrum taken from Ref. 5. The Fermi energy is indicated by a dotted line.

TABLE II. The calculated magnetic moments and f occupation numbers of SmZn . All symbols have the same meaning as in Table I.

U (Ry)	0.0	0/ $J=0$	0.2	0.4	0.5	0.6	0.6
$m_{\text{total}} (\mu_B)$	5.91	5.94	5.94	5.97	5.97	5.85	6.00
$m_{\text{orb}} (\mu_B)$	-2.29	-2.20	-3.46	-2.86	-2.88	-4.69	-2.82
$m_{\text{spin}} (\mu_B)$	5.16	5.22	5.20	5.55	5.52	4.82	5.58
n_{+1}	0.60	0.74	0.93	0.91	0.91	0.96	0.92
n_{+2}	0.58	0.69	0.56	0.90	0.89	0.03	0.91
n_{+3}	0.44	0.30	0.02	0.01	0.01	0.02	0.01
						stable	metastable

strained DFT method.) Since f electrons are strongly localized the common problem of the choice of the double counting recipe¹⁴ does not appear. The fully localized limit¹⁴ is to be applied.

III. RESULTS AND DISCUSSION

Detailed calculations have been carried out for a series of U values in both intermetallics. In choosing the U value we started from the theoretically determined U values and then chose the value which gave the correct f occupation numbers for Sm. We have done calculations for $U=0.0, 0.2, 0.4, 0.5,$

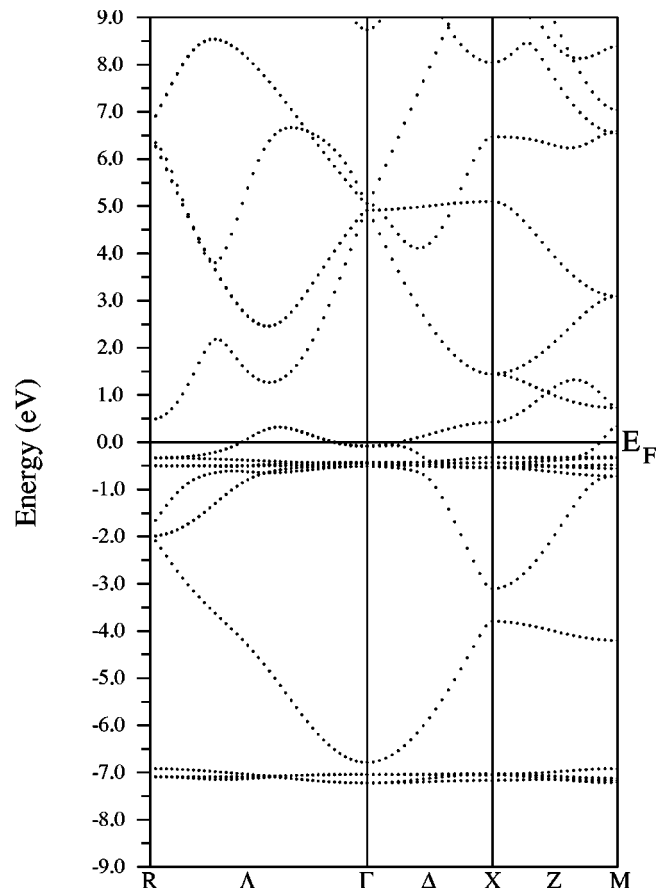


FIG. 5. The spin-up SmZn LSDA band structure.

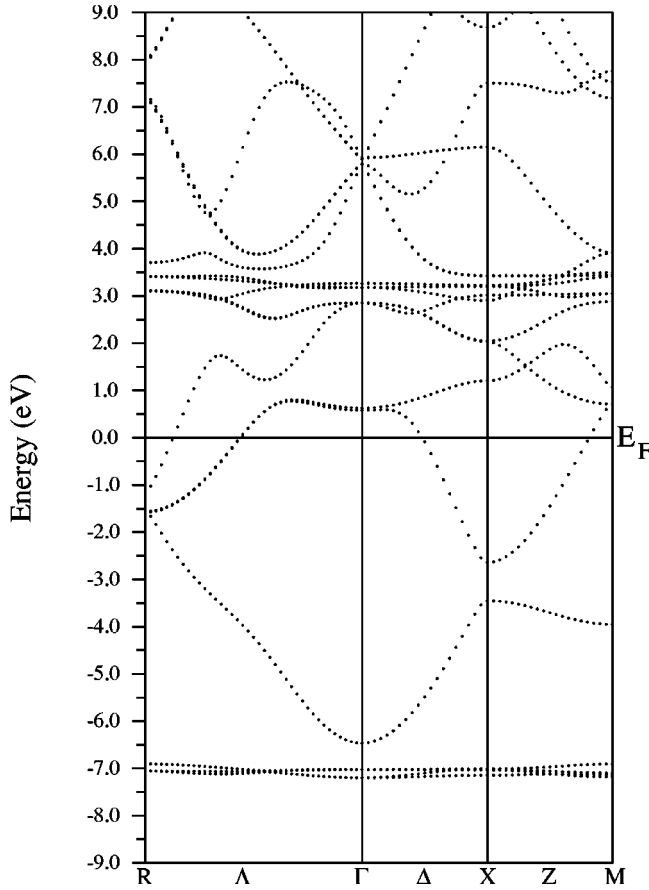


FIG. 6. The spin-down SmZn LSDA band structure.

and 0.6 Ry keeping constant the value of the exchange parameter J to 0.05 Ry. We have also done calculations with the LSDA+SO approach (which coincides with $U=J=0$).

A. SmAl₂

The f occupation numbers for Sm are collected in Table I together with the calculated magnetic moments. We observe that the appropriate Hubbard U parameter for SmAl₂ is $U \geq 0.5$ Ry since for this value we were able to stabilize the correct f electron occupancies, corresponding to the electron configuration of the Sm ion which is close to $4f^5$. The spin and the orbital magnetic moments of Sm ion are, respectively, $m_{\text{spin}} = 5.34\mu_B$ and $m_{\text{orb}} = -2.37\mu_B$ in the LSDA+SO. When the LSDA+ U +SO with $U=0.5$ Ry is applied, they become $m_{\text{spin}} = 4.94\mu_B$ and $m_{\text{orb}} = -4.78\mu_B$. These values compare well with the moments derived from the measured thermomagnetic curves $m_{\text{spin}} \approx -3.8\mu_B$ and $m_{\text{orb}} \approx 4.3\mu_B$, respectively.¹ The two opposite oriented components of the magnetic moment are comparable in magnitude and almost cancel out. The Coulomb correlation effects, which enlarge the $4f$ level splitting and increase the orbital magnetic moment, are obvious. Such a large orbital magnetic moment indicates that Sm $4f$ states are localized in SmAl₂.

As shown in Fig. 1, LSDA+SO calculations incorrectly pin all the spin-up states of the f orbitals in a sheath around

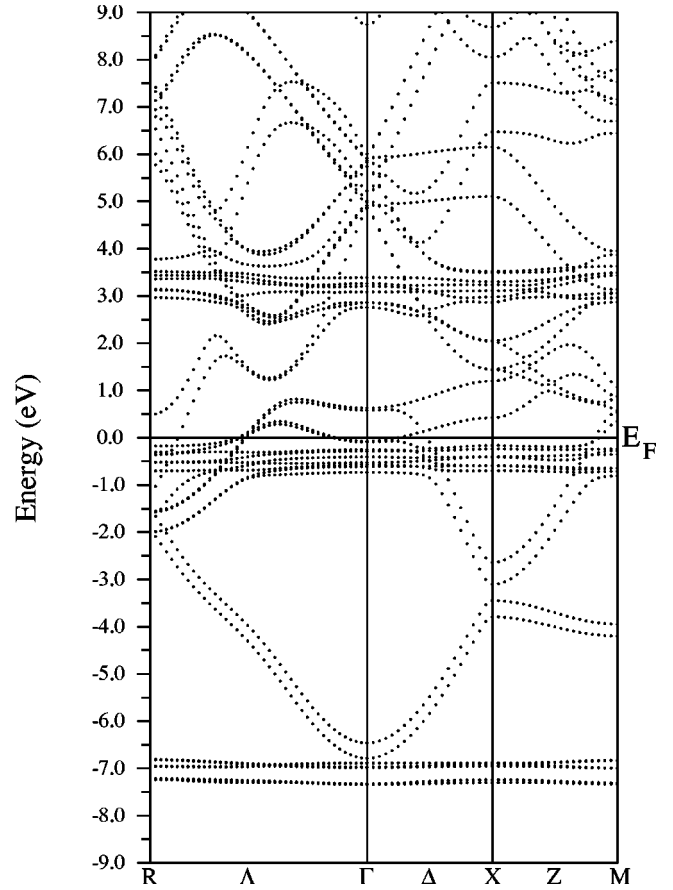


FIG. 7. Calculated band structure of SmZn with the LSDA+SO approach.

the Fermi energy. LDA+ U circumvents this problem by including a Hubbard U correction to the f orbitals, which naturally splits the f bands into lower and upper Hubbard bands with nearly integer occupancies (Fig. 2). As Fig. 2 shows the effects of including the on-site Coulomb interaction between the Sm $4f$ orbitals are the shift of the occupied $4f$ bands towards higher binding energies and the shift of the unoccupied $4f$ bands further away from the Fermi energy. The spin-up f band structure shows the seven split subbands and the Fermi level is close to the second spin-up Sm f subband. From the decomposition of f charge one can identify the crystal field splittings in the spin-up band structure of SmAl₂.

Figure 3 presents the spin-up SmAl₂ band structure, obtained from the LSDA+ U calculation in the ferromagnetic ground state. In the band structure, the Sm d character is indicated by the relative size of the plotting symbols. The spin-up band structure shows that the flat bands near 4 and 6 eV are heavily dominated by Sm d states. The largest contribution to the Fermi level comes from the Sm f electrons with a small contribution from Sm d electrons.

To further examine the microscopic origin of the valence band electronic structure of SmAl₂, we have calculated the Sm partial f density of states (DOS) in the LSDA+ U +SO approximation. Figure 4 compares the experimental Sm $4f$ PE spectrum to the calculated Sm $4f$ DOS. The theoretical

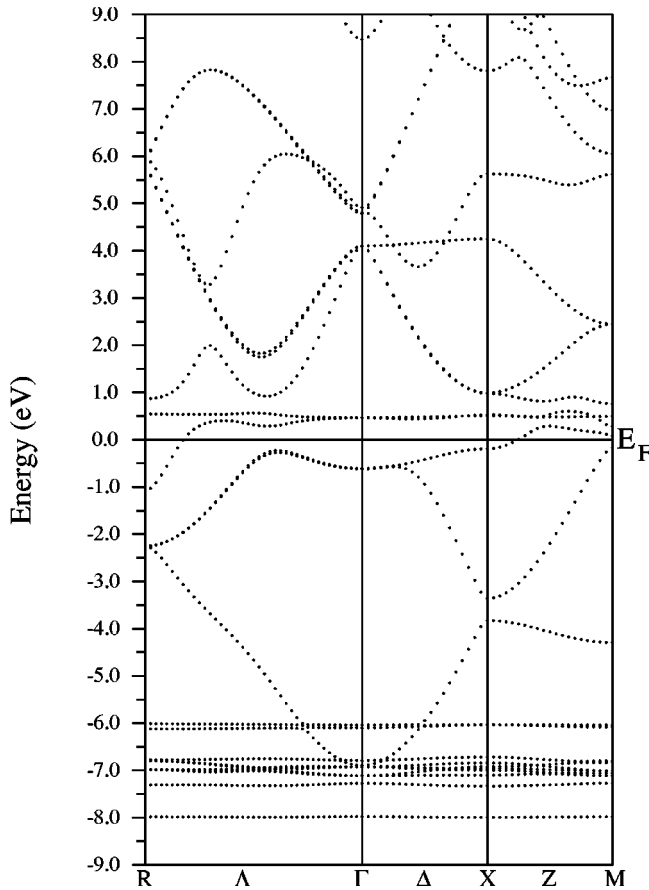


FIG. 8. The spin-up SmZn band structure, obtained from the LSDA+ U calculation.

curve is convoluted with a Gaussian function of 0.25 eV to simulate the instrumental resolution. It is observed that the trends in the PE spectrum are in good agreement with those in the LSDA+ U +SO calculation. In the calculated valence DOS the position and the height of the peak around -5.4 eV are in very good agreement with the PE peak. However, for the small emission near -7.4 eV the peak height is only in fair agreement.

B. SmZn

The f occupation numbers for Sm are collected in Table II together with the calculated magnetic moments. We observe that the appropriate Hubbard U parameter for SmZn is $U \geq 0.6$ Ry since for this value we have the correct f electron occupancies. The spin and the orbital magnetic moments of Sm ion are, respectively, $m_{\text{spin}} = 5.22\mu_B$ and $m_{\text{orb}} = -2.20\mu_B$ in the LSDA+SO. When the LSDA+ U +SO is applied, they become $m_{\text{spin}} = 4.82\mu_B$ and $m_{\text{orb}} = -4.69\mu_B$, causing spin-orbital compensation. These values compare well with the moments derived from the measured thermomagnetic curves $m_{\text{spin}} \approx 3.6\mu_B$ and $m_{\text{orb}} \approx -4.0\mu_B$, respectively.¹

Since the LDA+ U correction is always negative for occupied orbitals and positive for unoccupied ones, if during

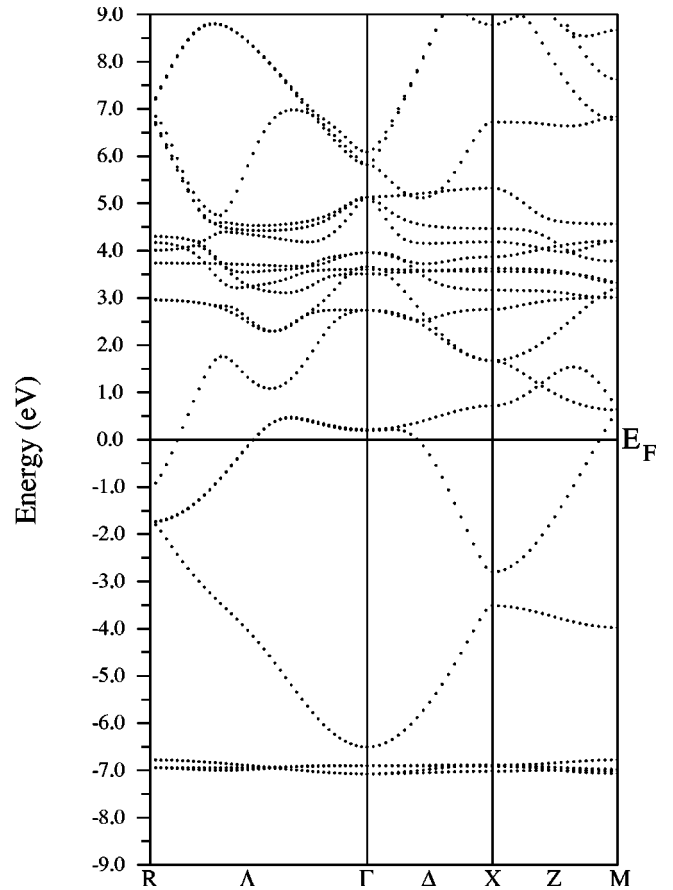


FIG. 9. The spin-down SmZn band structure, obtained from the LSDA+ U calculation.

the self-consistency process the system has some states occupied and other ones unoccupied then if the on-site Coulomb repulsion is large it will never change occupancies and metastable local minimum solutions are found.

One can obtain many different LDA+ U solutions depending on the starting charge density (and density matrix). As Table II shows, in SmZn there are metastable solutions at least for $U = 0.6$ Ry (the stable one has the correct f electron occupancies and the lowest total energy). Calculations with larger U 's are even more prone to produce such spurious metastable solutions, so extreme care should be taken not to mistake them for the ground state.

Figures 5 and 6 show the spin-up and down LSDA band structures obtained from LSDA+ U calculations with $U = J = 0$. It is shown that the valence band extends from E_F to about 7 eV below E_F , in both of them. In Fig. 5 there are very flat bands at ~ -0.5 eV corresponding to Sm 4*f* majority electrons (up). Similarly, in Fig. 6 the flat portions of the band structure curves between 3 and 4 eV correspond to Sm 4*f* minority electrons (down). In both Figs. 5 and 6 there are flat bands at ~ -7 eV, whose low dispersion can be attributed to the strong localization of the Zn 3*d* electrons. The spin-orbit interaction couples the spin-up and down states, as Fig. 7 shows.

Figures 8 and 9 present the spin-up and down bands obtained from LSDA+ U calculations. The parameters used in

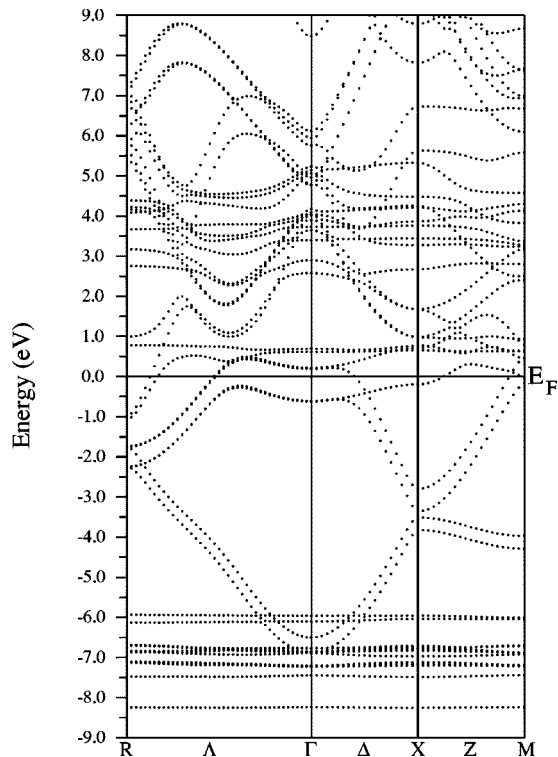


FIG. 10. Calculated band structure of SmZn with the LSDA + U + SO approach.

these calculations are the Coulomb correlation $U=0.6$ Ry and the exchange $J=0.05$ Ry for the Sm $4f$ electrons. Comparison with Fig. 5 shows that in the LSDA + U approximation, the spin-up Sm $4f$ bands disappear near E_F by the

Coulomb correlation interaction. The unoccupied spin-up Sm $4f$ bands shift up a little bit away from the Fermi energy, whereas the occupied spin-up bands are pushed down to between 6 and 8 eV below E_F and remain as local levels. Similarly, comparison with Fig. 6 shows that the spin-down Sm $4f$ bands are pushed up to between 3 and 5 eV above E_F . The Zn $3d$ bands obtained from the LSDA + U calculation are the same as those from the LSDA calculation, indicating a mixing between the occupied spin-up bands of Sm $4f$ and the Zn $3d$ bands at ~ -7 eV (see Fig. 8). Again the spin-orbit interaction couples spin-up and down states, so they are no longer separable (Fig. 10).

IV. SUMMARY

We found that the LSDA + U method can give physically meaningful description of spin-orbital compensation in Sm intermetallics. The method is not parameter free and the appropriate Hubbard U parameter is between 0.5 and 0.6 Ry. For large U 's, characteristic for the f -shell metals, the LSDA + U functional is liable to have a number of metastable magnetic solutions depending on the starting density matrix. Therefore, extreme care should be taken to identify the true ground state and not a metastable solution.

ACKNOWLEDGMENTS

We are grateful to P. Blaha, D. J. Singh, and P. Larson for useful conversations and advice. This work was supported by the Office of Naval Research. The work of H.J.G. was supported by the National Research Council Associateship Program.

*Present address: Department of Physics and Astronomy, CSUN, 18111 Nordhoff Street, Northridge, CA 91330-8268.

¹H. Adachi, H. Ino, and H. Miwa, Phys. Rev. B **59**, 11 445 (1999).

²H. Adachi and H. Ino, Nature (London) **401**, 148 (1999).

³H. Adachi, H. Kawata, H. Hashimoto, Y. Sato, I. Matsumoto, and Y. Tanaka, Phys. Rev. Lett. **87**, 127202 (2001).

⁴J.W. Taylor, J.A. Duffy, A.M. Bebb, M.R. Lees, L. Bouchenoire, S.D. Brown, and M.J. Cooper, Phys. Rev. B **66**, 161319(R) (2002).

⁵C. Laubschat, G. Kaindl, W.-D. Schneider, B. Reihl, and N. Martensson, Phys. Rev. B **33**, 6675 (1986).

⁶V.I. Anisimov, J. Zaanen, and O.K. Andersen, Phys. Rev. B **44**, 943 (1991); A.I. Liechtenstein, V.I. Anisimov, and J. Zaanen, *ibid.* **52**, R5467 (1995).

⁷I.V. Solovyev, A.I. Liechtenstein, and K. Terakura, Phys. Rev. Lett. **80**, 5758 (1998).

⁸V.I. Anisimov, I.V. Solovyev, M.A. Korotin, M.T. Czyzyk, and G.A. Sawatzky, Phys. Rev. B **48**, 16 929 (1993).

⁹D.J. Singh, *Planewaves, Pseudopotentials and the LAPW Method* (Kluwer Academic, Boston, 1994).

¹⁰P. Blaha, K. Schwarz, G.K.H. Madsen, D. Kvasnicka, and J. Luitz, *WIEN2k, An Augmented Plane Wave + Local Orbitals Program for Calculating Crystal Properties*, K. Schwarz, Technische Universität Wien, Austria, 2001.

¹¹J. Kunes, P. Novak, R. Schmid, P. Blaha, and K. Schwarz, Phys. Rev. B **64**, 153102 (2001).

¹²J.P. Perdew, K. Burke, and M. Ernzerhof, Phys. Rev. Lett. **77**, 3865 (1996).

¹³P. Larson, I.I. Mazin, and D.A. Papaconstantopoulos, Phys. Rev. B **67**, 214405 (2003).

¹⁴A.G. Petukhov, I.I. Mazin, L. Chioncel, and A.I. Liechtenstein, Phys. Rev. B **67**, 153106 (2003).